Return maps of folded nodes and folded saddle-nodes

John Guckenheimer
Mathematics Department, Cornell University, Ithaca, New York 14853, USA

(Received 3 August 2007; accepted 4 September 2007; published online 27 March 2008)

Folded nodes occur in generic slow-fast dynamical systems with two slow variables. Open regions of initial conditions flow into a folded node in an open set of such systems, so folded nodes are an important feature of generic slow-fast systems. Twisting and linking of trajectories in the vicinity of a folded node have been studied previously, but their consequences for global dynamical behavior have hardly been investigated. One manifestation of the twisting is as "mixed mode oscillations" observed in chemical and neural systems. This paper presents the first systematic numerical study of return maps for trajectories that flow through a region with a folded node. These return maps are approximated by rank-1 maps, and the local twisting of trajectories near a folded node gives rise to multiple turning points in the approximating one dimensional maps. A variant of the forced van der Pol system is used here to illustrate that folded nodes can be a "chaos-generating" mechanism. Folded saddle-nodes occur in generic one-parameter families of slow-fast dynamical systems with two slow variables. These bifurcations give birth to folded nodes. Numerical simulations demonstrate that return maps of systems that are close to a folded saddle-node can be even more complex than those of folded nodes that are far from folded saddles.
[DOI: 10.1063/1.2790372]

Multiple time scales give rise to dynamical phenomena that are different from those seen in generic vector fields with a single time scale. This paper examines the "global" dynamics that are associated with two such phenomena; namely, folded nodes and folded saddle-nodes. These folded singularities occur in the context of systems with two slow variables. Folded nodes are typical in such systems: they occur in open sets of such systems, and open regions of trajectories flow to folded nodes. Previously, stable and unstable slow manifolds of the folded nodes have been studied. These manifolds twist around a "principal canard" trajectory and their intersections are secondary canards. This paper presents numerical investigations of the flow map between two cross sections that lie on opposite sides of a folded node. It finds that this map is a perturbation of a one-dimensional map. The approximating one-dimensional map has apparent discontinuities at the secondary canards turning points where its behavior is no longer determined by the folded nodes themselves and it has turning points in between. Combined with a global return to the original cross section, the nonmonotonic structure of the flow map can generate chaotic dynamics. This is illustrated with an example that is a modification of the forced van der Pol equation. Folded saddle-nodes are codimension one bifurcations of systems with two slow variables that give rise to folded nodes. Numerical computations find additional complexity of the flow maps of folded saddle-nodes.

I. INTRODUCTION

Slow-fast vector fields have the form

$$\varepsilon\dot{x} = f(x,y,\varepsilon), \quad \dot{y} = g(x,y,\varepsilon) \tag{1}$$

with $x \in R^m$ the fast variable, $y \in R^n$ the slow variable, and ε a small parameter that represents the ratio of time scales. The dynamics of these systems is shaped by the interactions of the two time scales. The critical manifold C of the system is defined by $f=0$ and consists of equilibria of the layer equations or fast subsystems $\dot{x}=f(x,y,0)$. The variable y acts like a parameter in the layer equations. Where the equilibria of the fast subsystems are hyperbolic, there is an invariant slow manifold of system (1) that lies close to the critical manifold.[8] The folds of the critical manifold consist of the points where $D_x f$ is singular, and hence the tangent space of C fails to be transverse to the subspace parallel to x coordinates. The equation $\dot{y}=g(x,y,0)$ can be projected onto the tangent plane of the critical manifold off the fold curve to give the vector field $(-(D_x f)^{-1} D_y f g, g)$. This vector field on the critical manifold can be rescaled to extend to fold points, producing the slow flow of the critical manifold. Write $(D_x f)^{-1}$ as $(\det D_x f)^{-1}(D_x f)^{\dagger}$ (Cramer's rule), to obtain the slow flow $(\pm(D_x f)^{\dagger} D_y f g, \mp(\det D_x f) g)$. The signs in the slow flow are chosen so that the orientation of the slow vector field agrees with the full vector field near stable sheets of the critical manifold. The choice depends upon whether m is even or odd. The y component of this slow flow vanishes on the fold curve. Points where $\pm(D_x f)^{\dagger} D_y f g \neq 0$ on the fold curve are said to satisfy the normal crossing conditions. The slow flow has equilibrium points on the fold curve where the normal crossing conditions fail.

Consider now the case of two slow variables, i.e., $n=2$, and one fast variable, i.e, $m=1$. The critical manifold is two-dimensional and the folds form a curve. The matrix $D_x f$ is a scalar, and the slow flow is given by $(D_y f g, -D_x f g)$, a vector field tangent to the critical manifold. Points of the fold curve where $D_y fg=0$, but $g \neq 0$ are called folded singularities or pseudosingularities. The folded singularities can be classified as equilibria of the slow flow: the terms "folded nodes," "folded foci," and "folded saddles" are used to describe those with real nonzero eigenvalues of the same sign, complex eigenvalues with nonzero real parts, and eigenvalues of opposite sign, respectively. Folded saddle-nodes occur where a folded singularity has a zero eigenvalue. They occur in generic one-parameter families of systems with two slow variables. Normal forms (or systems of first approximation[1]) can be defined for folded singularities and used to study the local flows of the full systems (1) in neighborhoods of the folded singularities,[1,9,15] though there are fewer results about equivalence of systems to their normal forms than is the case with equilibria of systems with a single time scale. The flows of the normal forms are surprisingly complex. This paper adds to our understanding of vector fields with folded nodes and folded saddle-nodes by describing effects of these structures on return maps and invariant sets.

Hyperbolic folded singularities are open in the space of C^2 slow-fast systems with two slow variables and one fast variable. Moreover, an open region of slow flow trajectories are asymptotic to a folded node, as noted already by Takens.[17] In the full system (1), all trajectories that flow into the vicinity of a folded-node emerge from that region: there is no invariant set in a small neighborhood of the folded node. Consequently, one expects to encounter folded nodes in generic periodic orbits and other attractors of these slow-fast systems. The objective of this work is to determine how the local flow near the folded node influences the properties of attractors passing through this region. Folded saddle-nodes are a codimension-1 bifurcation of slow-fast systems that give rise to folded nodes in systems with two slow variables and one fast variable. Thus, flow maps through the region of folded saddle-nodes are important in understanding the attractors of generic one-parameter families of slow-fast systems. This paper does not attempt a thorough analysis of these flow maps, but it highlights some of their complex dynamics.

II. FOLDED NODES

A. A normal form

The following equations are a normal form or system of first approximation[1] for folded nodes in systems with two slow variables and one fast variable:

$$\varepsilon \dot{x} = y - x^2, \quad \dot{y} = -x - z, \quad \dot{z} = b, \tag{2}$$

where $0 < b < 1/8$. Low-order Taylor expansions of general three-dimensional systems with a folded node can be reduced to this form by coordinate changes.[20] Further scaling of the coordinates (x,z,t) by $\sqrt{\varepsilon}$ and y by ε eliminates ε from Eq. (2) producing the scaled system

$$X' = Y - X^2, \quad Y' = -X - Z, \quad Z' = b. \tag{3}$$

The slow flow of system (2) is

$$\dot{z} = 2bx, \quad \dot{x} = -x - z. \tag{4}$$

The dynamics of the system (2) were studied by Benoit[2–4] and later by Szmolyan and Wechselberger,[16] Wechselberger,[20] and Guckenheimer and Haiduc.[10] Benoit observed that there are a pair of algebraic solutions to Eq. (2) that include canards; i.e., trajectories that remain close to the critical manifold for all time. He also observed that other canards are possible in the system: these "secondary canards" spiral around one of the primary canards. Guckenheimer and Haiduc[10] showed that the number of these secondary canards is unbounded as $b \to 0$ and Wechselberger[20] studied their bifurcations. In all of this work, the emphasis is upon the canards and upon the properties of the slow stable and unstable manifolds as they approach the canard region. Here we investigate the flow maps that describe how trajectories entering a neighborhood of the folded node exit that region. Note that no trajectories remain in the vicinity of the folded node for all time because $\dot{z}=b$ is a positive constant.

B. Normal form dynamics and flow maps

In the singular limit $\varepsilon=0$, the normal form of the folded node [Eq. (2)] is an algebraic-differential equation in which motion is constrained to its critical manifold $y=x^2$. Consider trajectories with initial conditions that lie far from the critical manifold in the case $\varepsilon > 0$ small. These trajectories first flow almost parallel to the x axis, quickly reaching an ε neighborhood of the critical manifold or infinity. Near the critical manifold, motion is approximated by the slow flow defined by the system (4). The slow flow is linear with negative eigenvalues $-1/2 \pm \sqrt{1-8b}/2$. Both its eigendirections lie in the second and fourth quadrants of the (z,x) plane with the weaker eigenvector lying closer to the z axis. Trajectories of the slow flow with initial conditions in the second quadrant sector bounded by the lines $x=0$ and $z=(-1/2-\sqrt{1-8b}/2)x$ flow to the origin without encountering the fold curve $x=0$. The slow flow ceases to be a good approximation to the flow of the system (2) in a neighborhood of the origin of radius $O(\varepsilon^{1/2})$. The differences between these two systems are more readily seen by working with the rescaled system (3).

For large Y and $X>0$, the system (3) has an attracting slow manifold that lies close to the surface $Y=X^2$. There is an open region of trajectories that approach this slow manifold quickly and then follow it to the vicinity of the folded node at the origin. The variable Z increases linearly along the manifold. The part of the manifold with $Z<0$ develops spirals as it approaches the cross section $Z=0$. When it leaves this region, the spirals end. Figure 1(a) shows four of these trajectories with Fig. 1(b) showing an expanded view of their passage close to the origin. Desroches, Krauskopf, and Osinga[7,14] have produced elegant visualizations of the stable and unstable manifolds and their intersections.

Benoit[3] observed that the curves $(X,Y,Z)(t)=(\alpha t, \alpha + \alpha^2 t^2, bt)$ with $2\alpha^2+\alpha+b=0$ are solutions of the system (3). The variational equations describing the flow near one of these primary canards is a time varying linear system (the Weber equation) that has complex eigenvalues when $|\alpha t| = |X| < 1$. Wechselberger[20] used these variational equations to analyze the bifurcations producing secondary canards in

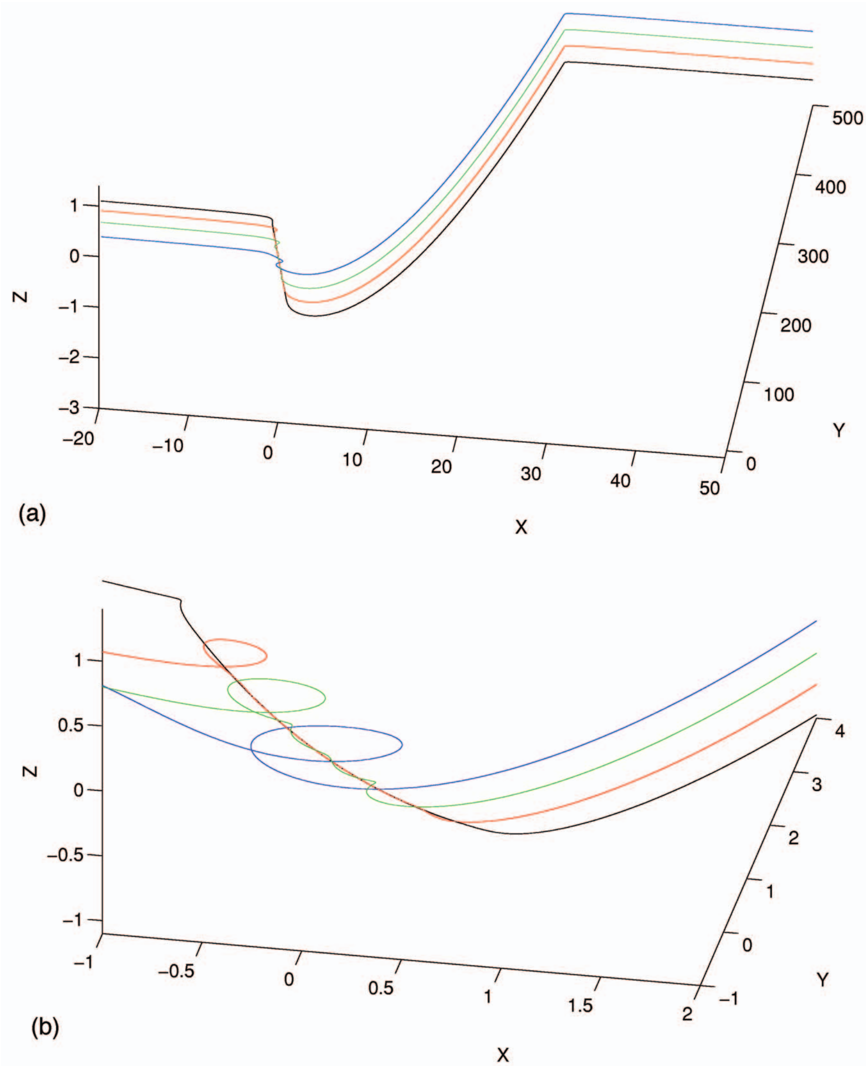

FIG. 1. (Color) (a) Four trajectories of system (3) that link each other as they pass through the region near the origin. The parameter $b=0.03$ Initial values are $(X,Y)=(50,500)$ and $Z \in \{-2.5,-2.18,-1.86,-1.54\}$. (b) A detailed view of the trajectories in the vicinity of the origin.

the system, determining the number of secondary canards in terms of the ratio μ of the eigenvalues for the slow flow [Eq. (4)]. This quantity is $O(b)$ as $b \to 0$. Brøns, Krupa, and Wechselberger[6] show that the secondary canards on the stable slow manifold are all within a distance $O(\varepsilon^{(1-\mu)/2})$ of the "strong" primary canard of system (2).

When b is also small, the system (2) can be studied as a three time scale system with ε the ratio of middle to fast time scale and b the ratio of slow to middle time scale. The system (3) becomes a slow-fast system with the two fast variables (X,Y) and the slow variable Z like the "tourbillon" studied by Wallet.[18] In the singular limit with Z acting as a parameter, the flow is described by the two-dimensional vector fields

$$X' = Y - X^2, \quad Y' = -X - Z, \tag{5}$$

where Z is now a parameter. These flows have a unique equilibrium point at $(X,Y)=(-Z,Z^2)$,which changes type as Z increases. The types are a stable node for $Z<-1$, a stable focus when $-1<Z<0$, a center when $Z=0$, an unstable focus when $0<Z<1$, and an unstable node when $1<Z$. Figure 2 shows phase portraits of these flows for $Z=-2$, $Z=-0.25$, and $Z=0$. Phase portraits for $Z>0$ are obtained by the time reversing symmetry $(X,Y,Z,T) \to (-X,Y,-Z,-T)$ of system (3). This time reversing symmetry also implies that the system (5) has a continuous family of periodic orbits when $Z=0$. The twisting and linking of the trajectories of system (2) are "explained" by the phase portraits of system (5) with focal equilibria for $|Z|<1$. Figure 1(b) plots segments of four trajectories close to the origin of system (3).

Yet a further consequence of the time reversing symmetry is that there is an unstable slow manifold of system (3) that is the symmetric image of the slow manifold. Figure 3 shows intersections of the slow stable and unstable manifolds with the plane $Z=0$. The intersections of these two manifolds lie on "maximal" canards that remain on the slow manifold for all time. Guckenheimer and Haiduc[10] showed that the number of these intersections is $O(1/b)$ (see also Refs. 18 and 20). The presence of several maximal canards indicates that the flow map through the region of a folded node is quite complicated. One of the principal contributions of this paper is to visualize the properties of this map.

We choose two cross sections to the scaled vector field [Eq. (3)], an initial plane S_1 defined by $X=50$ and a final plane S_2 defined by $X=-20$. Points in S_1 with $Y \gg 0$ approach the attracting slow manifold and then follow it to the

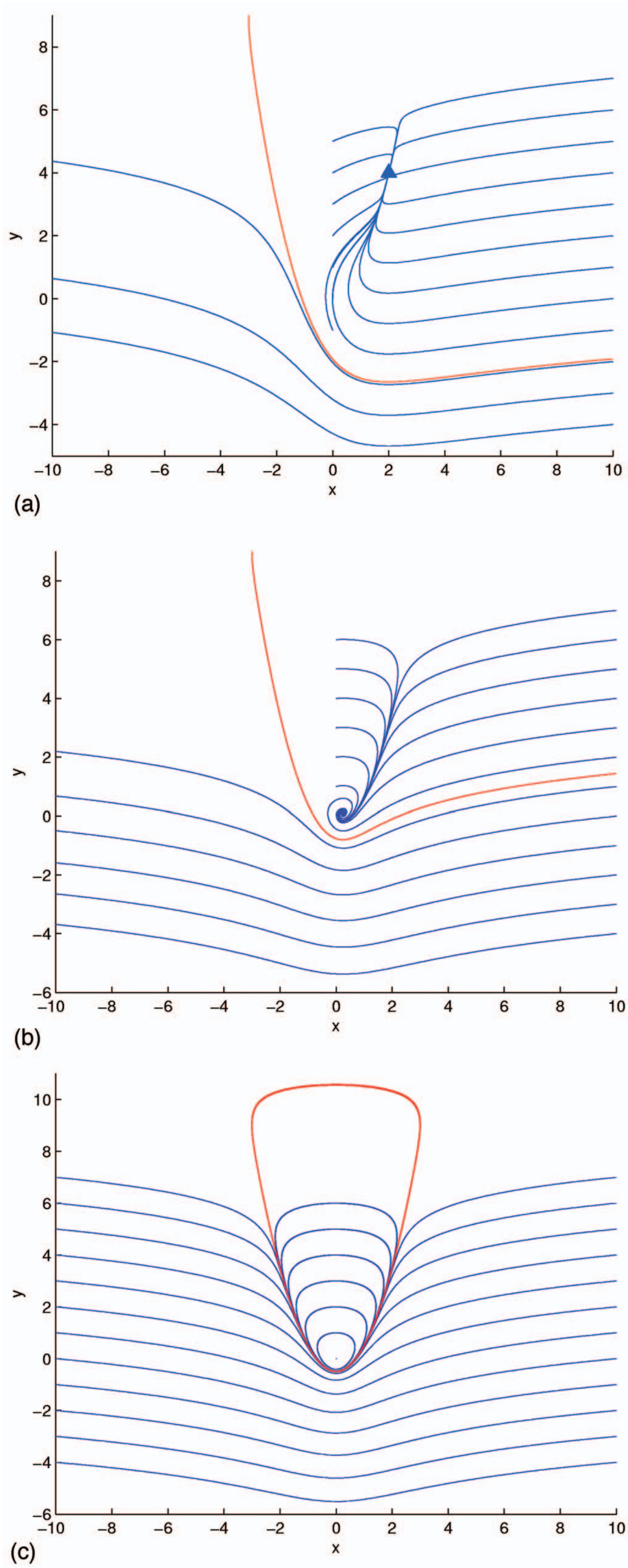

FIG. 2. (Color) Phase portraits of planar vector fields (5) for three different values of Z: (a) $Z=-2$, (b) $Z=0.25$, and (c) $Z=0$. In each case there is a single equilibrium point. The equilibrium is a stable node whose domain of attraction lies to the right and above the red trajectory in (a), a stable focus whose domain of attraction lies to the right and above the red trajectory in (b) and a center that is surrounded by a family of periodic orbits that lie above the parabola $Y=X^2-1/2$ in (c). Trajectories below this parabola and those below the red trajectories in (a) and (b) flow to infinity in finite time.

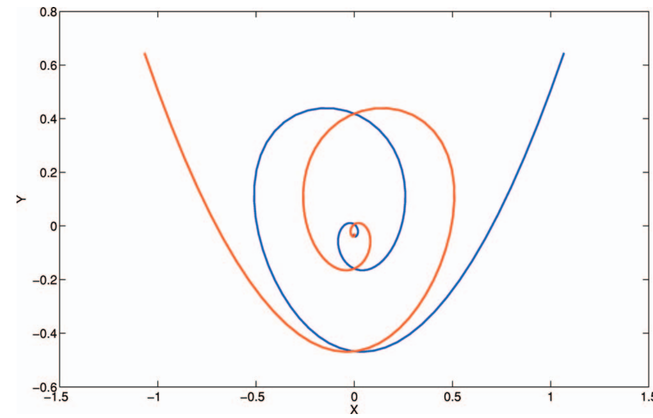

FIG. 3. (Color) Intersections of the slow stable and unstable manifolds of the system (3) with the plane $Z=0$. The parameter $b=0.03$. The stable manifold was computed by following 370 trajectories with initial conditions along a segment parallel to the Z axis to their intersections with this plane. The intersection of the unstable manifold with the plane $Z=0$ is the reflection of the stable manifold.

fold curve along the Z axis, as illustrated in Fig. 1(a). Because the flow contracts strongly onto the stable slow manifold, the image of the flow map F_{12} from S_1 to S_2 is close to a rank-1 map. Numerically, we choose a grid of points along a segment or two-dimensional mesh in S_1 and integrate the trajectories of these points to their intersection with S_2. Figure 4(a) shows the F_{12} image in S_2 of a rectangular 3×300 grid of points $X=50$, $Y\in 450,500,550$, $Z\in[-2.99,0]$ with parameter $b=0.03$. This value of b yields moderate numbers of maximal canards and twists in the slow manifolds. The points are colored red, blue, or green according to whether $Y=450$, 500, or 550. Note that the images of the three segments of initial conditions with varying X and fixed Y lie near a common set of curves, consistent with the flow map being approximated by a rank-1 map. More information about the flow map is shown in Fig. 4(b), which plots the final value of Z in terms of the initial value of Z for trajectories starting on the segment $Y=500$. There are seven apparent discontinuities in this map that occur near the maximal canards. This number of discontinuities is consistent with the results of Wechselberger[20] (cf. Ref. 6) that estimate the number of intersections of the slow stable and slow unstable manifolds in terms of the eigenvalues of the slow flow for the system. In this case ($b=0.03$), the eigenvalue is approximately $\mu=14.6$ and the estimate for the number of intersections of the manifolds is $1+[(\mu-1)/2]=7$. The canards separate trajectories with differing numbers of twists around the principal canard. The trajectories displayed in Fig. 1 come from different "branches" of this graph. Each branch between a pair of discontinuities in Fig. 4(b) corresponds to a segment of the blue slow stable manifold in Fig. 3 between successive intersections with the red slow unstable manifold. These are the sectors whose size is analyzed by Brøns, Krupa, and Wechselberger.[6] Since these segments begin and end on the slow unstable manifold, the time that it takes for the trajectory to reach S_2 is larger at the ends of the segment than in the middle. Because Z varies linearly with time, each branch of the graph shown in Fig. 4(b) has a local minimum. The presence of these local minima and the discontinuities

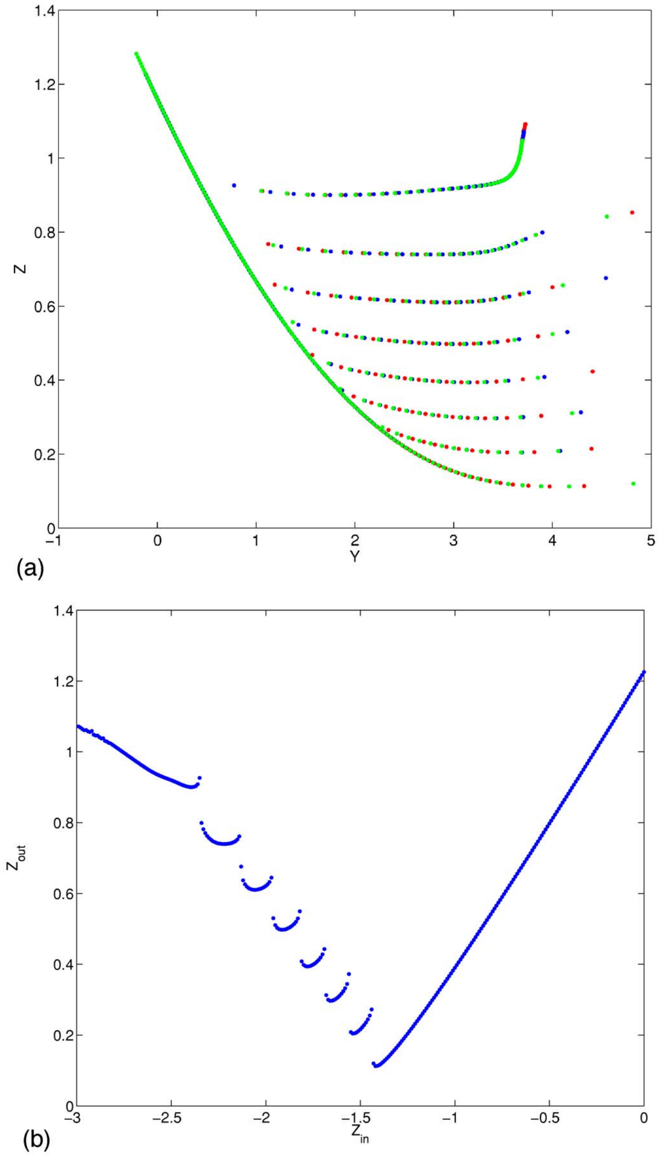

FIG. 4. (Color online) (a) The intersections of a grid of 3×300 trajectories with the plane $X=-20$. The initial conditions are equally spaced in the rectangle $X=50$, $Y \in [450,500]$, $Z \in [-2.99,0]$. The color of the points indicates the initial value of Y. (b) Graph of the final values of Z vs initial values of Z for the trajectories with initial value $Y=500$ shown in (a).

between branches suggest that folded nodes can serve as a chaos producing mechanism for three-dimensional systems with two slow and one fast variable. The next section gives an example that illustrates that this is indeed the case.

III. AN EXAMPLE: FOLDED NODES IN INVARIANT SETS

This section presents numerical simulations of the following system, a variant of the forced van der Pol system with folded nodes:

$$\varepsilon \dot{x} = y + x - \frac{x^3}{3}, \quad \dot{y} = -x + a\sin(2\pi\theta),$$
$$\dot{\theta} = b + \omega\left(1 - \frac{1}{1+(x^2-1)^2}\right). \tag{6}$$

Folded nodes occur in the forced van der Pol system[5,11] itself, but only over a small range of parameters close to values that produce a folded saddle-node. The scale of the dynamics associated with these folded nodes makes it difficult to resolve the twisting dynamics described in the previous section. The example introduced here expands the phase space region in which folded nodes influence the dynamics and it includes parameters that "tune" the number of twists made by trajectories entering the folded node. The slow flow of the system (6) is the system

$$x' = -x + a\sin(2\pi\theta),$$

$$\theta' = \left(b + \omega\left(1 - \frac{1}{1+(x^2-1)^2}\right)\right)(x^2-1).$$

There are folded singularities if $a \geq 1$ at points where $x = \pm 1$ and $\sin(2\pi\theta) = x/a$. If $0 < b\sqrt{a^2-1} < 1/16\pi$, then two of the four folded singularities are folded nodes. Small values of b produce folded nodes with lots of twisting.

Figure 5(a) displays a trajectory of the system (6) with parameters $(a,b,\omega,\varepsilon) = (1.24, 0.001, 0.5, 0.01)$ projected into the (x,θ) plane. The overall shape of the trajectory is similar to the relaxation oscillations of the forced van der Pol system. Trajectories follow a stable sheet of the slow manifold $y = x^3/3 - x$ to the fold curves at $x = \pm 1$, where they jump to the opposite sheet. However, the details of the jumps differ from jumps at fold points that satisfy the normal crossing condition because they occur near the folded nodes of the system. Figure 5(b) shows an expanded view of the trajectory near the fold curve at $x=-1$. The trajectory segment shown makes four passages through this region, and does not repeat its past trajectory on subsequent passages. The oscillations associated with the folded node are apparent.

The system (6) has the same symmetry $(x,y,\theta) \rightarrow (-x, -y, \theta+0.5)$ as the forced van der Pol system. Relying on this symmetry, we study the global behavior of the system via a half-return map that begins on the section $x=0$ in the middle of the jumps with $y \approx 2/3$ and integrates trajectories until they reach this section again (with $y \approx -2/3$) and then applies the symmetry to obtain a new point on the section with $y \approx 2/3$. Periodic orbits of the half-return map of period k come from periodic orbits whose projection to the (x,y) plane has winding number around the origin either k or $k/2$, dependent upon whether the symmetry maps the orbit into itself. Since there is strong contraction of the flow to the slow manifold, its half-return map can be approximated by a rank-1 map. The dynamics of the half-return map can be visualized by following the trajectories with initial conditions varying along the circle defined by $(x,y) = (0, 2/3)$ and plotting the final values of the θ coordinate versus its initial values. Figure 6(a) displays the θ coordinates of the half-return map for this system for a set of initial conditions on

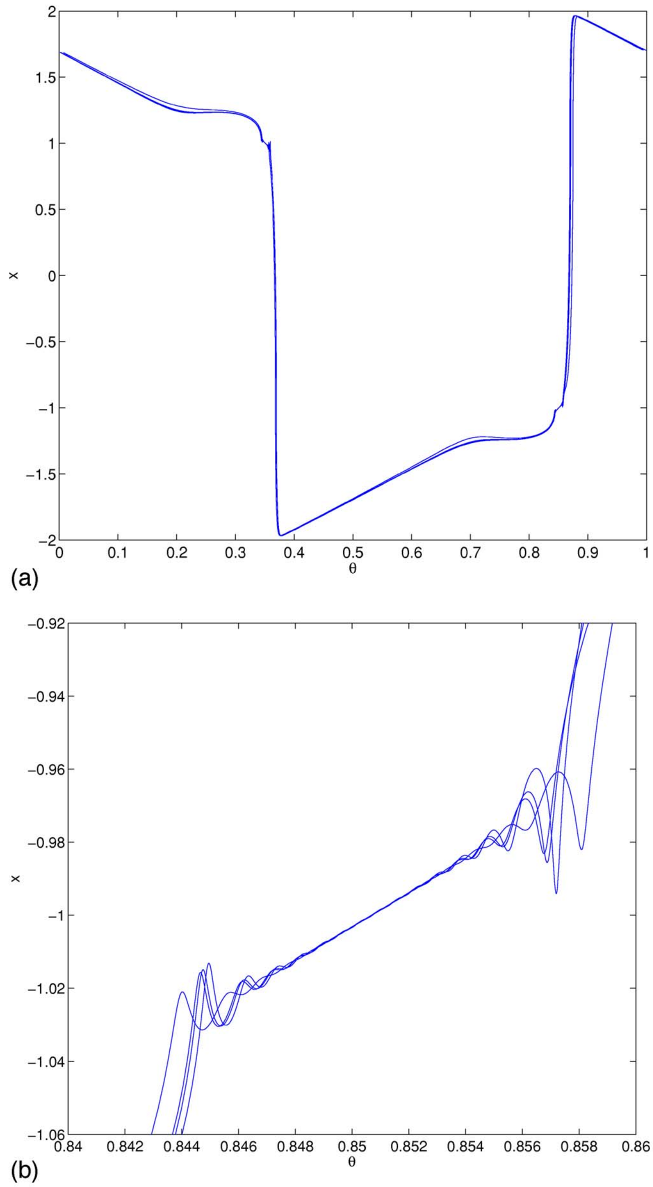

FIG. 5. (Color online) A trajectory of the system (6) that makes repeated returns to the vicinity of folded nodes. The initial conditions are $(x, y, \theta) = (0, 0.636\,668, 0.868\,822)$ and the parameter values are $(a, b, \omega, \varepsilon) = (1.24, 0.001, 0.5, 0.01)$.

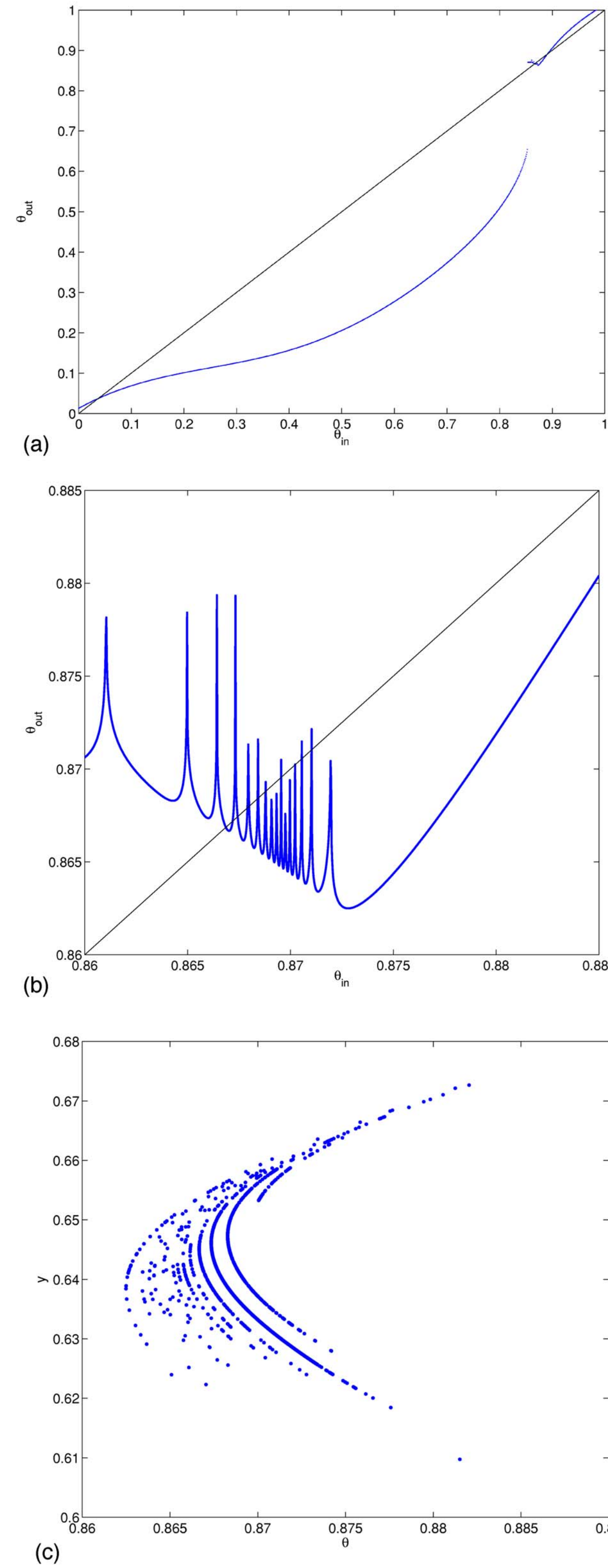

FIG. 6. (Color online) (a) Half-return map for the system (6). (b) Expanded view of a portion of the half-return map. (c) Poincaré map constructed from 2000 returns of the trajectory shown in Fig. 5 to the cross section $x=0$. The parameters are the same as those used in Fig. 5.

the circle $(x, y) = (0, 2/3)$. The apparent discontinuity in values of the half-return map occurs on the stable manifold of the folded saddle. Trajectories on one side of the discontinuity flow directly to the fold curve of the system where they jump to the opposite sheet of the slow manifold. Trajectories on the other side of the discontinuity turn away from the fold curve at the folded saddle and follow its unstable manifold to the vicinity of the folded node. The twisting near the folded node creates a small region where the return map is not monotone. A detailed view of this region is shown in Fig. 6(b).

The return maps shown in Figs. 6(a) and 6(b) resemble those of one-dimensional maps that are known to have chaotic attractors.[12] Figure 6(c) displays a Poincaré map of a trajectory for this system that further suggests that the system has a chaotic invariant set. Based on these computations, it is possible to formulate geometric hypotheses that imply the existence of chaotic invariant sets passing through neighborhoods of a folded node in a slow-fast system with two slow and one fast variable. Variations of the parameter b in the system (6) influence where trajectories flowing through the folded node return to the cross section, thereby producing bifurcations that create and destroy the chaotic invariant set whose cross section is illustrated in Fig. 6(c). In comparison with the forced van der Pol system, the chaotic invariant sets of this example appear to occupy larger regions of the parameter space and have larger cross-sectional area in the parameter space. Guckenheimer, Wechselberger, and Young[13] studied another modification of the forced van der Pol equation that has a different chaos generating mechanism that produces a sizable chaotic region of its parameter space. They prove that the theory of Henon-like chaotic attractors[19] applies to that example.

IV. FOLDED SADDLE-NODES

Folded saddle-nodes occur when a pair of folded singularities appear on the fold curve of a slow-fast system with two slow variables. The following system has a folded saddle-node at the origin when $\bar{a}=0$:

$$\varepsilon\dot{x} = y - x^2, \quad \dot{y} = -x + \bar{a} - z^2, \quad \dot{z} = \bar{b}. \tag{7}$$

It can be rescaled to

$$X' = Y - X^2, \quad Y' = -X + a - Z^2, \quad Z' = b \tag{8}$$

by setting

$$x = \sqrt{\varepsilon}X, \quad y = \varepsilon Y, \quad z = \varepsilon^{1/4}Z,$$
$$t = \sqrt{\varepsilon}T, \quad a = \bar{a}\varepsilon^{-1/2}, \quad b = \bar{b}\varepsilon^{1/4}. \tag{9}$$

Note that $ab^2 = \bar{a}\bar{b}^2$ remains unchanged by the scaling of ε. We may assume that $b>0$ in system (8) by changing the sign of Z if $b<0$. The slow flow of system (7) is

$$\dot{x} = -x + \bar{a} - z^2, \quad \dot{z} = 2\bar{b}x. \tag{10}$$

Folded singularities occur when $a>0$ in the system (7), and the magnitude of a determines their separation. For $\bar{a}>0$, the system (7) has a folded saddle when $x=y=0$, $z=-\sqrt{\bar{a}}$, and a folded node when $x=y=0$, $z=\sqrt{\bar{a}}$, $0<\bar{a}\bar{b}^2<\frac{1}{256}$. If $\bar{a}\bar{b}^2>\frac{1}{256}$, the folded singularity at $x=y=0$, $z=\sqrt{\bar{a}}$ is a folded focus.

Figure 7 shows the phase portrait of this slow flow for $(a,b)=(0.01,0.275)$. The trajectories along the segment of the fold curve $z=0$ flow upwards away from the fold curve. Thus the strip of trajectories between the stable manifold of the folded saddle and the strong stable manifold in the upper half of the (z,x) plane flow into the folded node. Outside of this strip the trajectories in the upper half of the (z,x) plane reach the fold curve where they jump without encountering the folded singularities. Note also that the maximal canards in this system are finite and do not extend to infinity because all the backward trajectories in the lower half-plane to the right of the unstable manifold of the folded saddle intersect the fold curve.

The complicated bifurcations of the folded saddle-node involve the formation of canard segments within the strip of trajectories that approach the folded node. The prominent bifurcations of these trajectories are those associated with canards that follow the unstable slow manifolds of the folded saddle and the folded node. Wechselberger[20] analyzed the normal form of a folded node, computing asymptotic formulae for these bifurcations. When a is large enough in system (8), the folded saddle and folded node are sufficiently separated that the bifurcation theory of the folded node applies without modification. As a decreases, the stable manifold of the folded saddle approaches and enters the region of trajectories that oscillate around the folded node. Trajectories close to the stable manifold of the folded saddle then oscillate around the folded node. Figure 8(a) shows the plot of final versus initial Z coordinates of F_{12} for parameters $(a,b)=(0.37,0.03)$. It is evident that the apparent discontinuity at the stable manifold of the folded saddle borders on the region where there are oscillations around the folded node. Figure 8(b) shows two trajectories on opposite sides of this apparent discontinuity associated with the folded saddle. Note that the trajectories immediately to the right of the folded saddle twist. The inward spiraling of the trajectory is far less symmetric with its outward spiraling than that displayed by the trajectories of the normal form for a folded node.

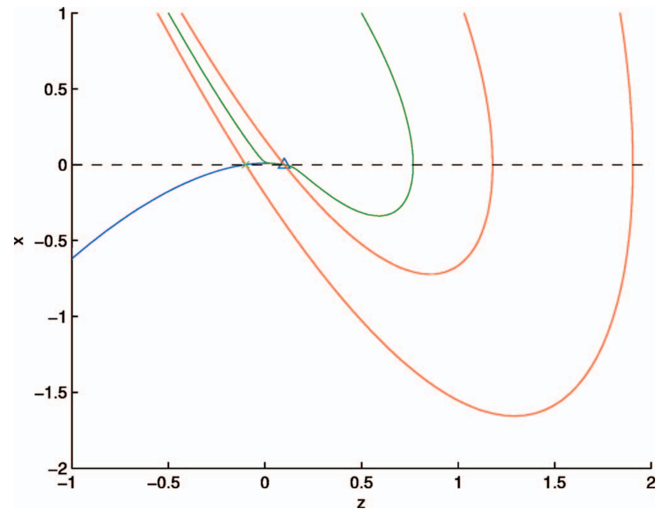

FIG. 7. (Color) Phase portrait of the slow flow equations (10). The parameters are $(a,b)=(0.01,0.275)$. The folded node is designated by a triangle and the folded saddle by a cross. The stable manifold of the saddle and the strong stable manifold of the node are red; the unstable manifold of the saddle is blue and additional pair of trajectories approaching the node are green. The fold curve is the dashed line $x=0$.

The discontinuities of the function displayed in Fig. 8(a) seem more complicated than the ones displayed by the corresponding function for the folded node bifurcation displayed in Fig. 4(b). In particular, the local minima of the branches close to the stable manifold of the folded saddle do not decrease monotonically as those of Fig. 4(b). Instead, there is an oscillation in their magnitudes. Figure 9(a) plots the projections of four trajectories onto the (X,Z) plane. These trajectories constitute two pairs that straddle the discontinuities of the second branch to the right of the stable manifold of the folded saddle. It appears that the trajectories in these regions are able to follow the unstable slow manifold of the folded node into the region where oscillations no longer occur, and that the trajectories from inside this branch jump "back" to the stable sheet of the slow manifold while

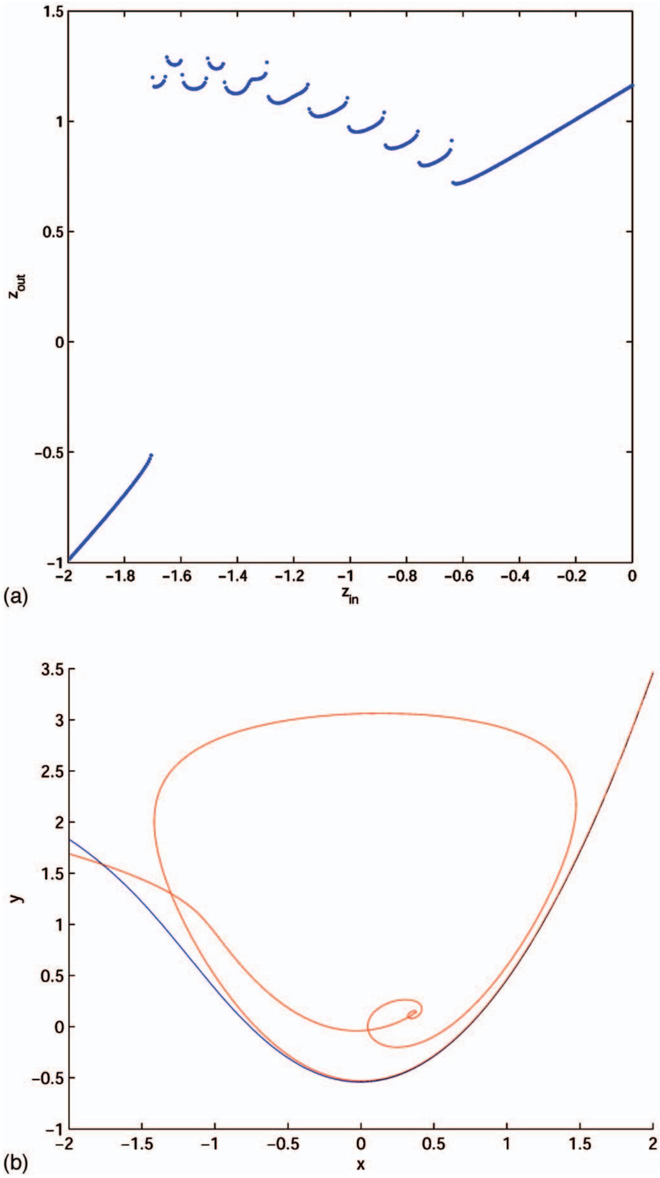

FIG. 8. (Color) (a) Image of the flow map F_{12} of system (8). Four hundred points along the segment $X=50$, $Y=400$, $Z \in [-2,0]$ are integrated to their intersection with $X=-10$. The Z coordinate of the final point is plotted against the Z coordinate of the initial point. (b) Trajectories of system (8) with initial conditions $(50,400,-1.705)$ and $(50,400,-1.7)$ projected into the (X,Y) plane.

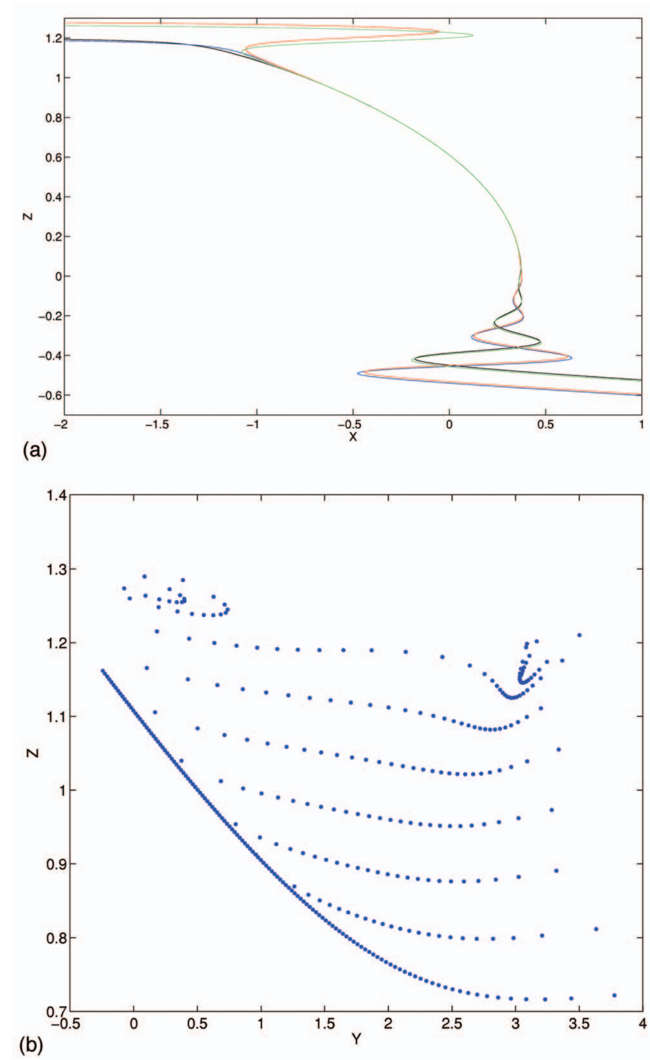

FIG. 9. (Color) (a) Four trajectories of the system (8). The initial conditions are $X=50$, $Y=400$, and $Z \in -1.655, -1.65, -1.6, -1.595$ colored blue, red, green, and black, respectively. The parameters are $(a,b)=(0.37,0.03)$. Note that the red and green trajectories that lie on the same branch of the flow map depicted in Fig. 8(a) jump back to positive values of X and reach the cross section $X=-2$ with larger values of Z than the other two trajectories. (b) Image of the flow map F_{12} of system (8). Four hundred points along the segment $X=50$, $Y=400$, $Z \in [-1.995,0]$ are integrated to their intersection with $X=-10$.

the trajectories on the other side of the discontinuity jump away from the slow manifold. The phase portraits of the two-dimensional flows depicted in Fig. 2 are relevant here. The separation of trajectories occurs at values of Z that correspond to the case $Z>1$ in system (5), where the two-dimensional flow has an unstable node rather than a focus. Figure 9(b) plots the image of the flow map of a segment of trajectories flowing through the region of the folded saddle-node, similar to Fig. 4(a). The branches in the upper part of this image also appear to be more complicated than those seem in Fig. 4(a). Further analysis of the flow maps associated to the folded saddle-node is not pursued here, but is clearly of interest.

V. CONCLUDING REMARKS

No theorems appear in this paper. Its purpose is to visualize novel aspects of the dynamical behavior produced by folded nodes in slow-fast systems with two slow variables and one fast variable. Given the complexity of these phenomena, analytic results that substantiate the numerical observations may be difficult to obtain. I conjecture that the main features visualized here for the flow maps through folded nodes are generic for such systems. Specifically:

- If the parameter b in the normal form [Eq. (2)] of a folded node is sufficiently small, then its return map will be approximated by a discontinuous one-dimensional map that has $O(1/b)$ branches, each of which is concave upward.
- The "slab" of trajectories giving rise to these branches has width $O(\sqrt{\varepsilon})$ in the direction parallel to the fold curve.[6]

- When the trajectories flowing through the folded node region return to this region, the twisting of trajectories can create chaotic invariant sets.

Additional bifurcations associated with secondary canards near a folded saddle-node have been visualized here, but the nature of these bifurcations and their dependence upon the parameters (a,b) in system (8) have not been investigated.

ACKNOWLEDGMENT

Research partially supported by the National Science Foundation and Department of Energy.

[1]V. I. Arnold, V. S. Afrajmovich, Yu. S. Il'yashenko, and L. P. Shil'nikov, *Dynamical Systems V*, Encyclopaedia of Mathematical Sciences (Springer-Verlag, Berlin, 1994).
[2]É. Benoît, "Systemes lents-rapides dans R^3 et leurs canards," *Third Schnepfenried Geometry Conference*, Schnepfenried (Soc. Math. France, Paris, 1982); [Asterisque **109–110**, 159 (1983)].
[3]É. Benoît, "Canards et enlacements," Publ. Math., Inst. Hautes Etud. Sci. **72**, 63 (1990).
[4]É. Benoît, "Perturbation singulire en dimension trois: canards en un point pseudo-singulier nœud," Bull. Soc. Math. France **129**, 91 (2001).
[5]K. Bold, C. Edwards, J. Guckenheimer, S. Guharay, K. Hoffman, Judith Hubbard, R. Oliva, and W. Weckesser, "The forced van der Pol II: Canards in the reduced system," SIAM J. Appl. Dyn. Syst. **2**, 570 (2003).
[6]M. Brøns, M. Krupa, and M. Wechselberger, "Mixed mode oscillations due to the generalized canard phenomenon," Fields Inst. Commun. **49**, 39 (2006).
[7]M. Desroches, B. Krauskopf, and H. M. Osinga, "The geometry of slow manifolds near a folded node," Research Report BCANM.991, University of Bristol, 2007.
[8]N. Fenichel, "Geometric singular perturbation theory," J. Differ. Equations **31**, 53 (1979).
[9]J. Guckenheimer, *Bifurcations of Relaxation Oscillations, in Normal Forms, Bifurcations and Finiteness Problems in Differential Equations*, edited by Y. Ilyashenko and C. Rousseau (Kluwer, Dordrecht, 2004), pp. 295–316.
[10]J. Guckenheimer and Radu Haiduc, "Canards at folded nodes," Mosc. Math. J. **25**, 91 (2005).
[11]J. Guckenheimer, K. Hoffman, and W. Weckesser, "The forced van der Pol equation I: The slow flow and its bifurcations," SIAM J. Appl. Dyn. Syst. **2**, 1 (2002).
[12]J. Guckenheimer and P. Holmes, *Nonlinear Oscillations, Dynamical Systems, and Bifurcations of Vector Fields* (Springer-Verlag, New York, 1983).
[13]J. Guckenheimer, M. Wechselberger, and Lai-Sang Young, "Chaotic attractors of relaxation oscillators," Nonlinearity **19**, 701 (2006).
[14]B. Krauskopf and H. M. Osinga, "Computing invariant manifolds via the continuation of orbit segments," in *Numerical Continuation Methods for Dynamical Systems*, edited by B. Krauskopf, H. M. Osinga, and J. Galan-Vioque (Springer, New York, 2007), pp. 117–154.
[15]E. Mishchenko, Yu. Kolesov, A. Kolesov, and N. Rozov, *Asymptotic Methods in Singularly Perturbed Systems* (Consultants Bureau, New York, 1994) (translated from the Russian by Irene Aleksanova).
[16]P. Szmolyan and M. Wechselberger, "Canards in R^3," J. Differ. Equations **177**, 419 (2001).
[17]F. Takens, "Constrained equations; a study of implicit differential equations and their discontinuous solutions," Lect. Notes Math. **525**, 143 (1976).
[18]G. Wallet, "Entre-sortie dans un tourbillon," Ann. Inst. Fourier **36**, 157 (1986).
[19]Q. Wang and L-S Young, "Toward a theory of rank one attractors," Ann. Math. (to be published).
[20]M. Wechselberger, "Existence and bifurcation of canards in R^3 in the case of a folded node," SIAM J. Appl. Dyn. Syst. **4**, 101 (2005).